Tellus (1982), *34*, 266–276

Baroclinic instability of a midlatitude zonal mean state changing with time

By TAKASHI SASAMORI, *Laboratory for Atmospheric Research, University of Illinois, 1101 W. Springfield Ave., Urbana, Illinois 61801, U.S.A.*

(Manuscript received May 18; in final form September 1, 1981)

ABSTRACT

A characteristic frequency equation is formulated for atmospheric Rossby waves embedded in a basic zonal mean state changing periodically with time, based on the two-layer model in the midlatitude β-plane. The characteristic frequencies are calculated for a truncated set of waves including up to the third higher harmonics of geopotential and temperature, and the results are compared with the classical baroclinic instability theory. The zonal mean thermal wind oscillating around the stationary state is found to be more unstable against small perturbations than the instability predicted by classical theory. The oscillating thermal wind influences the Rossby waves in two ways, firstly by enhancing the growth rate and secondly by modulating the propagation phase speed around the central phase velocity. The relative magnitudes of these two effects depend on the frequency and the amplitude of the changing thermal wind. On the other hand, the changing zonal mean wind mainly affects the phase speed of the Rossby waves with little influence on the growth rate. Using a highly truncated model it is shown that a resonant-type interaction is possible between the geopotential and the temperature wave modes in the perturbation when the zonal mean thermal wind changes periodically with time. It is suggested that the discrepancy often observed between the phase speed of developing Rossby waves on weather maps and classic baroclinic instability theory might be partly due to the changing zonal mean state with time.

1. Introduction

The dynamics of the baroclinic instability of the zonal mean thermal wind in midlatitudes is one of the successful theories in meteorology which contributed to progress in numerical weather forecasting, understanding the global general circulation and the genesis of fronts and cyclones. The linear theory by Charney (1947), Eady (1949) and Phillips (1954) is the basis of a number of subsequent developments of baroclinic instability analyses, and the essential features of the unstable Rossby wave are summarized in several standard texts, e.g., Holton (1972), Haltiner (1971), Pedlosky (1979). The largest growth rate occurs for the wave for which the wavelength is slightly larger than the Rossby radius of deformation; the growth rate is approximately proportional to the intensity of the zonally averaged thermal wind; the longiitudinal phase of the temperature wave lags behind the geopotential wave by approximately a quarter wavelength; and the wave as a whole propagates westward relative to the zonal mean flow. Although the theoretical prediction agrees well with the characteristics of developing weather systems in a sequence of daily weather maps, the phase speed and the propagation direction of developing cyclones and waves often deviate from the theoretical prediction. It is generally conceived that the nonlinearity of the actual atmospheric motions is largely responsible for the discrepancy, and most current numerical weather prediction theories are based on models which integrate the equations of motion without the assumption of small atmospheric disturbance amplitudes.

Among a number of possible nonlinear effects on unstable atmospheric motions, the effects of longitudinal inhomogeneity of atmospheric states have been analyzed by Lorenz (1972), Frederiksen (1978) and Lin (1980). However, the presence of

0040-2826/82/030266-11$02.50/0

stationary waves in the atmosphere does not significantly change the essential feature of the unstable waves (Frederiksen, 1978) since under normal conditions the baroclinic wave grows mainly at the expense of the available potential energy involved in the meridional gradient of the zonally averaged temperature, and the energy available from the longitudinal stationary temperature wave is rather small.

Another aspect of the nonlinear interaction of atmospheric wave motion and the zonal mean flow was studied by Matsuno (1971). The transport of momentum and heat by a transient planetary wave causes a change in the zonal mean motion which in turn influences the growth of the wave. Matsuno demonstrated numerically that this interaction may possibly cause sudden warming events in the winter stratosphere. Using a less general atmospheric model, Hirota (1971a,b) proposed a mechanism for the genesis of stratospheric transient planetary waves caused by the interaction between the changing zonal mean flow and forced Rossby waves which originate from stationary sources in the troposphere. His numerical analysis indicates that the amplitude of transient Rossby waves becomes largest at a certain period of the changing zonal mean flow, which is approximately 20 days. These analyses suggest that the changing zonal mean atmospheric condition influences planetary waves in two ways: firstly by changing the zonal mean potential energy available to the unstable waves, and secondly by modulating the propagation speed of the wave superimposed on the zonal mean flow.

In the troposphere, particularly in the winter high-latitudes, the zonal mean state is very variable with time. An example is shown in Fig. 1 for the difference of the zonal mean temperature between 45° and 85° N at 500 mb in winter 1963. The time change involves various time scales ranging from a slow seasonal progression to abrupt changes over a few days. The cause of changes occurring over short time periods may be due to intermittent events of baroclinic instability and also to the combined heat transport by the transient unstable wave and the statistically stationary waves forced by external sources (Madden, 1975). In any event, since the zonal mean energy potentially available to the Rossby waves is variable with time, it is likely that the characteristics of the unstable waves would be different from those predicted by classical

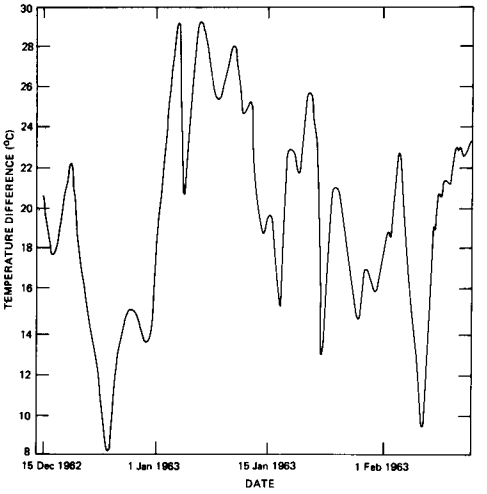

Fig. 1. Time change of difference of zonal mean temperature between 45° N and 85° N during winter 1962–63 at 500 mb.

baroclinic instability theory, particularly when the representative period in the changing zonal mean state is comparable to the e-folding time of the potentially unstable wave.

In this paper the characteristic frequency equation is formulated for a two-layer model using the quasi-geostrophic approximation in the midlatitude β-plane, with the zonal mean basic state prescribed by a simple periodic function of time, and a truncated number of characteristic frequencies is calculated by means of a boundary value problem.

2. Perturbation equation

Quasi-geostrophic wave motions in the two-layer midlatitude β-plane model may be governed approximately by the vorticity equation

$$\nabla^2 \psi_t + U\nabla^2 \psi_x + U_T \nabla^2 \phi_x + \beta\psi_x = 0 \qquad (2.1)$$

and the thermal vorticity equation

$$\nabla^2 \phi_t - \lambda\phi_t + U(\nabla^2 \phi_x - \lambda\phi_x) + U_T(\nabla^2 \psi_x + \lambda\psi_x) + \beta\phi_x = 0, \qquad (2.2)$$

where t denotes time, x and y are the horizontal Cartesian coordinates directing east and north respectively, ∇^2 is the horizontal Laplacian operator, and the suffixes t and x mean partial

differentiation with respect to those variables (Haltiner, 1971).

ψ is the geostrophic streamfunction at 500 mb, ϕ the geostrophic streamfunction for the thermal horizontal wind, β the meridional gradient of the Coriolis parameter, and the parameter λ is defined by

$$\lambda = \frac{f_0^2}{2g\sigma\Delta p}, \tag{2.3}$$

where f_0 is the Coriolis parameter at fixed latitude, g the gravitational constant, $2\Delta p$ the elementary pressure thickness of the two-layer model equal to 500 mb, and σ denotes the vertical static stability defined by

$$\sigma = \frac{\Delta p}{[\bar{\theta}]} \frac{\partial [\bar{z}]}{\partial p} \frac{\partial [\bar{\theta}]}{\partial p}, \tag{2.4}$$

where z is the geopotential height, θ the potential temperature and the overbar and the bracket indicate the time and zonal averages respectively. U and U_T are the zonal mean horizontal wind and thermal wind, which is proportional to the meridional gradient of zonal mean temperature. Both U and U_T have been assumed to be independent of y, but variable with time.

Since β and λ are the only constant external parameters of the model it is convenient to rewrite (2.1) and (2.2) in nondimensional form using the following time and horizontal length scales:

$$\text{time scale} = \lambda^{1/2}/\beta, \tag{2.5}$$

$$\text{horizontal length scale} = \lambda^{-1/2}. \tag{2.6}$$

The scale for the horizontal wind is subsequently defined by

$$\text{velocity scale} = \beta/\lambda. \tag{2.7}$$

The equation in nondimensional form has turned out to be formally the same as (2.1) and (2.2) except that λ and β are set equal to unity. We shall use the same symbols as defined for the dimensional equations. The scales of time, length and velocity are given in Table 1 for several latitudes.

Let us prescribe the time change of the zonal mean state by a single Fourier harmonic component superimposed on a stationary basic state:

$$U = A_0 + Ae^{i\mu t} + \tilde{A}e^{-i\mu t}, \tag{2.8}$$

$$U_T = B_0 + Be^{i\mu t} + \tilde{B}e^{-i\mu t}, \tag{2.9}$$

Table 1. *The scales for the nondimensional equation for representative latitudes*

Latitude	Horizontal length scale (km)	Time scale (day)	Velocity scale (m/s)
15	1640	0.332	57.1
30	843	0.693	14.1
45	583	1.226	5.5
60	469	2.163	2.5
75	415	4.720	1.0

where μ is a non-zero real number representing the nondimensional frequency, A_0 and B_0 are the stationary zonal wind and the thermal wind, and A and B are the amplitudes, which are generally complex. The over-tilde denotes the complex conjugate.

With these zonal mean states changing with time, the general solution for (2.1) and (2.2) must have the form:

$$\psi = \sum_{n=-\infty}^{\infty} \psi_n = e^{i(kx+ly)} \sum_{n=-\infty}^{\infty} X_n e^{in\mu t - \nu t}, \tag{2.10}$$

$$\phi = \sum_{n=-\infty}^{\infty} \phi_n = e^{i(kx+ly)} \sum_{n=-\infty}^{\infty} Y_n e^{in\mu t - \nu t}, \tag{2.11}$$

where k and l are nondimensional wavenumbers in the x and y directions, ν is the complex characteristic frequency and X_n and Y_n ($n = 0, \pm 1, \pm 2, \ldots$) are the complex expansion coefficients. By substituting (2.10) and (2.11) into (2.1) and (2.2), multiplying the result with $e^{-in\mu t}$ and then integrating over a period $2\pi/\mu$ we obtain

$$\mathbf{P}\boldsymbol{\xi}_{n+1} + \mathbf{Q}_n \boldsymbol{\xi}_n + \mathbf{R}\boldsymbol{\xi}_{n-1} = 0 \tag{2.12}$$

where

$$\boldsymbol{\xi}_n = \begin{pmatrix} X_n \\ Y_n \end{pmatrix}, \tag{2.13}$$

$$\mathbf{P} = \begin{pmatrix} k\tilde{A} & k\tilde{B} \\ \gamma k\tilde{B} & k\tilde{A} \end{pmatrix}, \tag{2.14}$$

$$\mathbf{Q}_n = \begin{pmatrix} \nu_G + n\mu - \nu & kB_0 \\ \gamma k B_0 & \nu_T + n\mu - \nu \end{pmatrix}, \tag{2.15}$$

$$\mathbf{R} = \begin{pmatrix} kA & kB \\ \gamma k B & kA \end{pmatrix}, \tag{2.16}$$

$$\nu_G = kA_0 - k\beta/(k^2 + l^2), \tag{2.17}$$

$$v_T = kA_0 - k\beta/(k^2 + l^2 + \lambda), \tag{2.18}$$

$$\gamma = (k^2 + l^2 - \lambda)/(k^2 + l^2 + \lambda), \tag{2.19}$$

with $\lambda = \beta = 1$.

The effect of changing the zonal mean state is contained in **P** and **R**. If the basic state is stationary ($A = B = 0$), the characteristic frequency is obtained by setting the determinant of $\mathbf{Q}_n$ equal to zero:

$$v = n\mu + (v_G + v_T)/2 \pm \{(v_G - v_T)^2 + 4\gamma k^2 B_0^2\}^{1/2}/2 \tag{2.20}$$

$(n = 0, \pm 1, \pm 2, \ldots)$.

By substituting this into (2.10) and (2.11) we see that all the solutions (ψ_n, ϕ_n) have the same complex phase velocity independent of μ as predicted by the classical baroclinic instability, i.e., the instability is possible when

$$(v_G - v_T)^2 + 4\gamma k^2 B_0^2 < 0. \tag{2.21}$$

By solving (2.21) in terms of $(k^2 + l^2)$ we obtain

$$\{1 - (1 - B_0^{-2})^{1/2}\}/2 < (k^2 + l^2)^2 < \{1 + (1 - B_0^{-2})^{1/2}\}/2. \tag{2.22}$$

This inequality has a physical meaning only if

$$B_0^2 \geqslant 1. \tag{2.23}$$

Equation (2.22) with (2.23) is the instability condition of a stationary zonal mean thermal wind B_0 against a small perturbation with wavenumbers k and l. When B_0 is only slightly larger than unity, the wavenumber of the unstable solution is limited to a narrow spectrum near

$$k^2 + l^2 \approx 1/\sqrt{2}. \tag{2.24}$$

To solve (2.12) numerically it is necessary to truncate the number of unknown eigenfunctions. The accuracy of the solutions depends on the number of unknowns retained in the equation, and increases with increasing n. Also the increase of n produces new eigenfunctions in addition to the solutions obtained by low-order truncation. The rate of convergence toward the accurate solution has been discussed in several papers for a similar recurrence equation for scalar variables (Lorenz, 1972; Gill, 1974; Tung, 1976). According to these analyses we may estimate the rate of convergence by a matrix

$$\mathbf{r} = \boldsymbol{\xi}_n \boldsymbol{\xi}_{n-1}^{-1}. \tag{2.25}$$

In a crude approximation **r** may be estimated by neglecting $\boldsymbol{\xi}_{n+1}$ in (2.12) as

$$\mathbf{r} = \mathbf{R}\mathbf{Q}_n^{-1}, \tag{2.26}$$

which may be written as

$$\mathbf{r} = \begin{pmatrix} kA(v_T + n\mu - v) & kB(v_T + n\mu - v) \\ -\gamma k^2 BB_0 & -k^2 AB_0 \\ -\gamma kB(v_G + n\mu - v) & kA(v_G + n\mu - v) \\ -\gamma k^2 AB_0 & -\gamma k^2 BB_0 \end{pmatrix} / \det \mathbf{Q}_n, \tag{2.27}$$

where

$$\det \mathbf{Q}_n = (v_T + n\mu - v)(v_G + n\mu - v) - \gamma k^2 B_0^2 \tag{2.28}$$

Roughly speaking, the numerator is of the order of $n\mu$ for large n and the denominator is proportional to $n^2\mu^2$, provided that all other parameters are of the order of unity, so that the magnitude of **r** decreases with increasing n. However, it is difficult to estimate the rate of convergence precisely, because it also depends on v, the eigensolutions of the recurrence equation. In particular, the discrete increase of new eigensolutions with increasing n makes it difficult to estimate (2.27). Therefore we show only a numerical example for a typical set of parameters as a basis for the truncation used in the analysis. In Figs. 2 and 3, the positive imaginary part of the eigenfrequency is shown as a function of the variable parameter μ, for $A_0 = A = 1$, $B = B_0 = 1.2$, $k = l = 0.5$. Fig. 2a shows the solution obtained by a truncation of harmonics with $|n| > 1$, while Fig. 2b shows the solution by a truncation of higher harmonics with $|n| > 2$. We see that the eigensolutions with largest growth rate are not very much different for these two sets of computations, but in Fig. 2b three new eigenfrequencies with smaller growth rate are calculated for individual μ. If we increase further the number of recurrence equations by truncating the higher harmonics with $|n| > 3$ (Fig. 3a) and $|n| > 4$ (Fig. 3b), the number of eignsolutions increases, particularly for small μ. But the eigenfrequencies with largest growth rate hardly change with increasing number of recurrence equations. Even the lowest order triad with only $n = 0$ and ± 1 produces fairly accurate solutions with largest growth rate. This numerical example suggests that the truncated solutions with

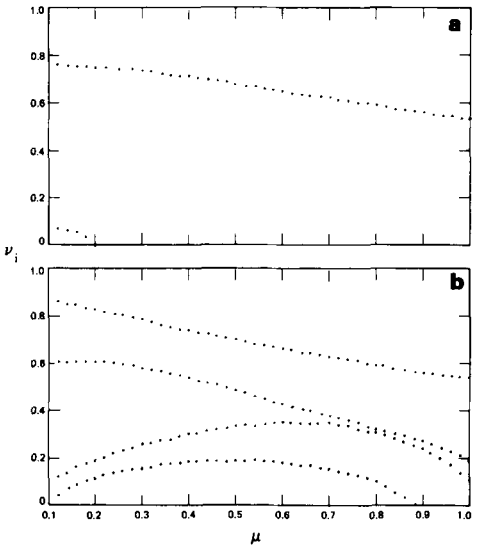

Fig. 2. Positive imaginary part of the eigenfrequency as a function of the frequency of changing thermal wind $A_0 = A = 1$, $B_0 = B = 1.2$, $K = l = 0.5$. (a) The harmonics with $|n| > 1$ truncated. (b) The harmonics with $|n| > 2$ truncated.

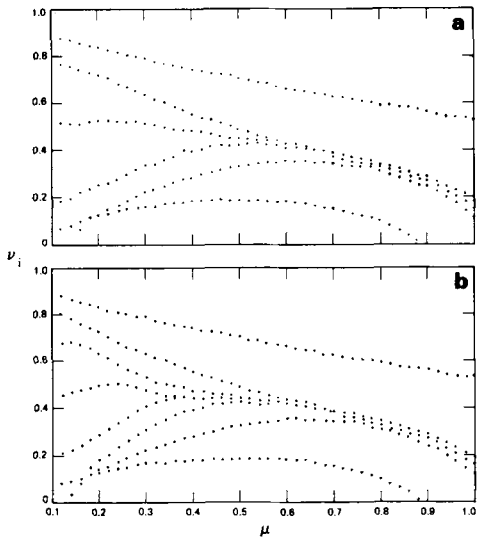

Fig. 3. Same as Fig. 2, except: (a) The harmonics with $|n| > 3$ truncated; (b) The harmonics with $|n| > 4$ truncated.

a limited number of harmonics are useful approximations for the qualitative analysis.

3. Characteristic solutions

The approximate solution of (2.12) was calculated by truncating the waves with $|n| > 3$ by a standard program available at the computer facility for 14 unknown eigenfunctions and eigenfrequencies. The fixed parameters were assumed to be

$$k = l = 0.5, \tag{3.1}$$

$$A_0 = 1. \tag{3.2}$$

Other parameters are summarized in Table 2.

Table 2. *Variable parameters used in the numerical calculations; $A_0 = 1$ for all cases*

Case	B_0	A	B
a	1.2	0	0
b	0	0	0.6
c	0	0	1.2
d	1.2	1.0	0.6
e	2.5	0	0
f	1.2	0	0.6
g	1.2	0	1.2
h	1.2	1.0	1.2
i	1.2	1.0	0
j	2.5	1.0	0
k	2.5	2.0	1.2

For the first set of computations (group I), $\mu = 0.2$, which corresponds to a dimensional period $2\pi/\mu \approx 1$ month in midlatitudes. For the second set of computations (group II), $\mu = 1.0$, which corresponds to a dimensional period equal to about a week in midlatitudes. $k = l = 0.5$ satisfies the instability condition (2.23) for both $B_0 = 1.2$ and 2.5 assumed in the computation, which will be referred to as the weakly and strongly unstable basic atmospheres, respectively.

The result for the slowly changing zonal mean state is summarized in Fig. 4, where the absolute value of the eigenfunction of the geopotential X_n is plotted as a function of the characteristic longitudinal phase velocity relative to a fixed point on the earth, defined by

$$c_r = (\nu_r - n\mu)/k, \tag{3.3}$$

where ν_r is the real part of the eigenfrequency. The growth rate of the unstable solutions with non-zero positive imaginary part is indicated by different symbols and the magnitude is shown by the numerical figures in the diagram. The magnitude of

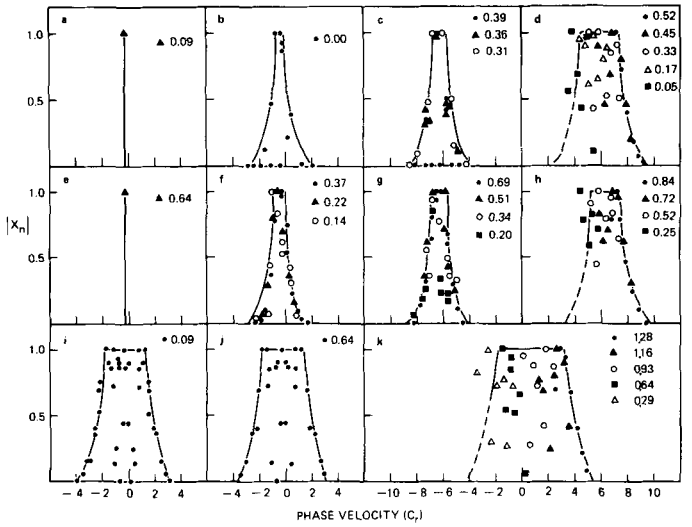

Fig. 4. Eigenfunction of the geopotential as a function of the phase velocity relative to a fixed point on the earth. The different marks indicate the eigenfunction with different imaginary parts of the frequency, the numerical figures being shown in the diagram. $k = l = 0.5$. Group I with $\mu = 0.2$. For other parameters, see Table 2.

the eigenfunctions is given by a relative scale with a normalization such that the largest value among the seven geopotential eigenfunctions belonging to each individual eigenfrequency is unity. The profile of the band envelope is shown by the solid line. The profile is only to show a rough range of broadening, and it is not accurate particularly where the distribution of eigenfunctions is highly discrete with a large gap as shown by the broken line.

Figs. 4a and 4e show the line spectrum of the classical baroclinic instability for the weakly and strongly unstable cases, respectively. Figs. 4b and 4c show the solutions when the basic zonal mean thermal wind slowly oscillates around the mean value, $B_0 = 0$. With $B = 0.6$ there is no unstable solution, but the phase velocity of the neutral stable wave is slightly dispersed around the central phase velocity. With $B = 1.2$, unstable waves with three different growth rates are possible with different phase velocities. The dispersion is slightly larger than when $B = 0.6$; in cases (f) and (g) it is assumed that $B_0 = 1.2$, otherwise it is the same as (b) and (c) respectively. Compared to (b) and (c), both the number of unstable solutions and the growth rate have increased, but the broadening of the phase velocity is about the same.

The effect of the changing zonal mean wind is shown in Figs. 4i and 4j. The growth rates of the unstable wave are the same as in the classical model, but a number of additional unstable waves with different phase velocities are produced.

In Figs. 4d, 4h and 4k, the results are shown for the cases when both A and B are changing with time simultaneously. It is seen from the figures that the broadening of the phase velocity is mainly due to variations in A and that the growth rates are determined primarily by B_0 and B.

The results computed with $\mu = 1.0$ are summarized in Fig. 5. A notable difference from Fig. 4 is that the dispersion of the phase velocity becomes larger when $\mu = 1$, whereas the growth rate of the unstable waves becomes smaller. In Fig. 4, there are a number of unstable solutions with the phase velocity close to the central value, but when μ is large many unstable waves propagate with phase velocities which are quite different from those predicted by classical theory.

Figs. 6 through 9 show the positive solution of the imaginary part of the characteristic frequency as a function of the frequency of the oscillating zonal mean temperature. $A_0 = 1$, $B = 0.6$ and $A = 0$ for all cases. When B_0 is smaller than the critical amplitude (2.23), the largest growth rate attains a maximum at a certain value of μ (Figs. 6 and 7). The reason will be discussed in Section 4. Fig. 8 shows that when B_0 is marginally unstable, the

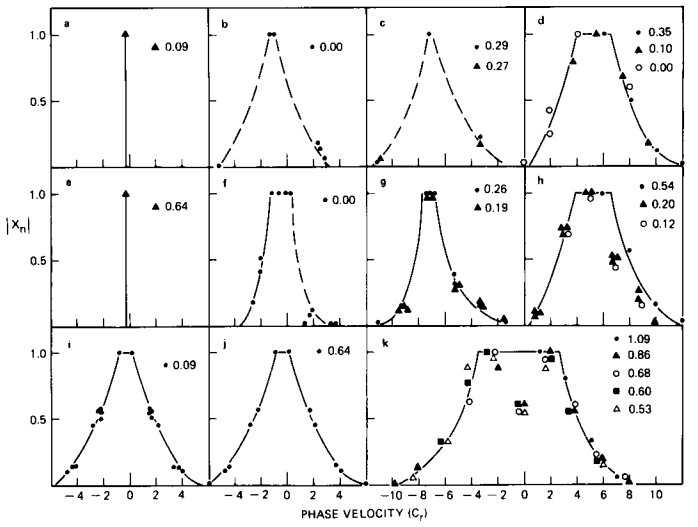

Fig. 5. Same as Fig. 4, except for Group II with $\mu = 1.0$.

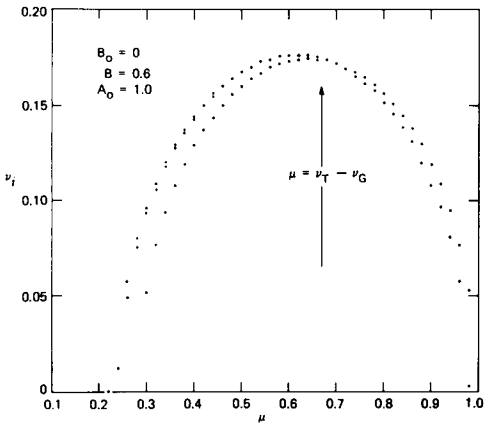

Fig. 6. Rate of growth of unstable waves given by the imaginary part of the characteristic frequency, as a function of the frequency of changing zonal mean thermal wind. $A_0 = 1$, $B_0 = 0$, $B = 0.6$, and $k = l = 0.5$ are assumed.

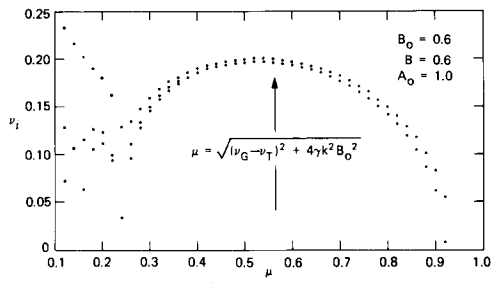

Fig. 7. Same as Fig. 6 except $B_0 = 0.6$.

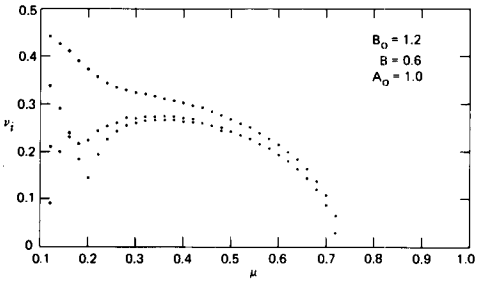

Fig. 8. Same as Fig. 6 except $B_0 = 1.2$.

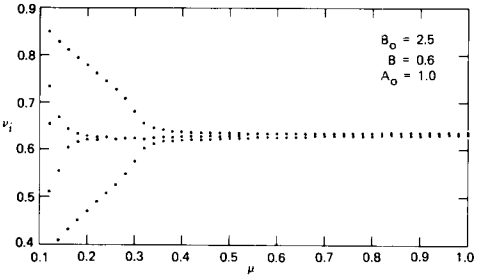

Fig. 9. Same as Fig. 6 except $B_0 = 2.5$.

additional effect of B increases the total growth rate when μ is small but decreases the growth rate when μ approaches unity. When the basic stationary state is strongly unstable (Fig. 9), the oscillating zonal mean temperature has little effect on the growth rate except when μ is small.

In all the numerical examples above, an isotropic perturbation ($k = l = 0.5$) has been assumed. To

estimate the effect of changing zonal mean thermal wind on the spectral range of unstable waves, the eigenfrequency computations were made by changing the wavenumbers k and l. One of the obvious shortcomings in the approximation using the midlatitude β-plane is the lack of proper boundary conditions at large y. In the actual atmosphere the dimension and the spherical shape of the globe and the boundary condition at the pole must influence the characteristics of the planetary wave (Frederiksen, 1978), and therefore the disturbances with very small l may not be realized in the atmosphere. In fact, nearly isotropic k and l is a good approximation as pointed out by Charney (1971). Nevertheless we assumed that l is variable over any range, just to give a perspective to the numerical result

The upper three diagrams in Fig. 10 show the largest positive imaginary parts of ν as a function of k and l, for $\mu = 0.3$, 0.6 and 0.9, respectively. $B_0 = B = 0.6$, $A_0 = 1$, $A = 0$ were assumed. Although the growth rate with a specific k becomes large when l decreases, the results with very small l may not have practical meaning because of the inaccurate β-plane approximation. The figure shows that the spectral range of the unstable waves is not very sensitive to the value of μ. The range for nearly isotropic disturbances ($k \approx l$) is about 0.5.

In the lower diagrams of Fig. 10 are shown the largest positive imaginary parts of ν for a case with $B_0 = 1.2$, $B = 0.6$, $A_0 = 1$, $A = 0$. In the same diagram the spectral range of instability (2.22) is also shown (shaded strip). It is seen that the changing thermal wind superimposed on the stationary state significantly increases the spectral range of the instability, particularly into the long wavelengths.

4. Approximate analytic solutions

To facilitate the interpretation of the previous numerical results, some approximate analytic solutions will be presented here for a simplified model by further truncating the waves with $|n| >$

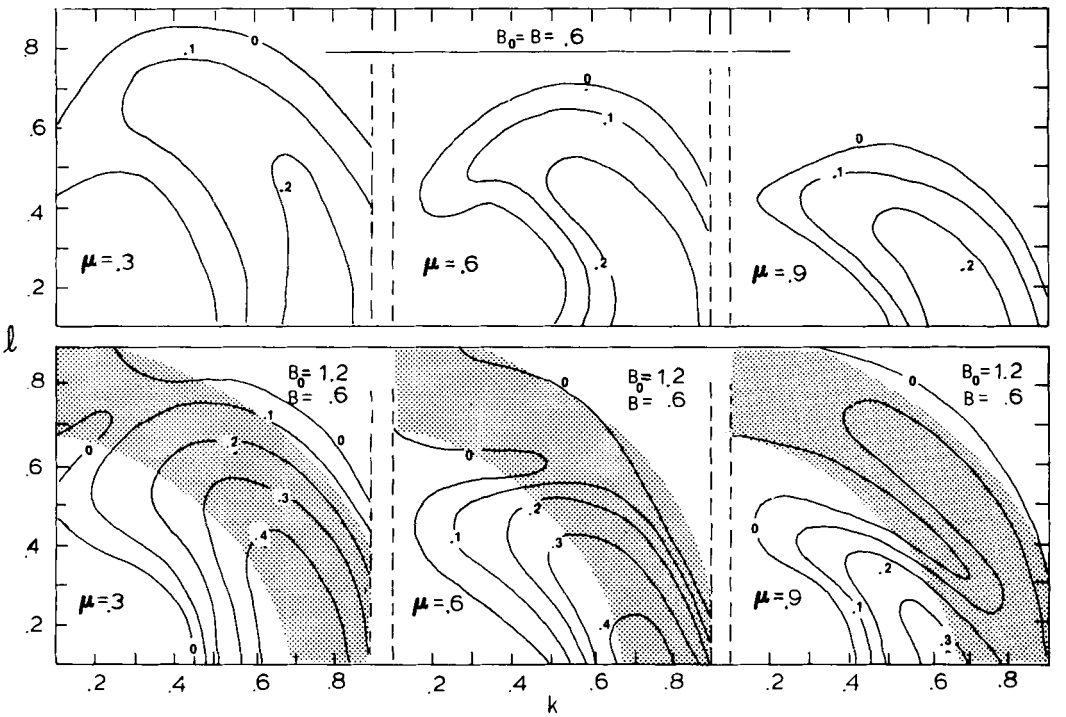

Fig. 10. The largest positive imaginary part of ν as function of k and l. Top: $B_0 = B = 0.6$, $A_0 = 1$, $A = 0$. Bottom: $B_0 = 1.2$, $B = 0.6$, $A_0 = 1$, $A = 0$. The instability range with $B_0 = 1.2$ alone is shaded.

1. In light of the numerical examples shown in Figs. 2 and 3, we assume that the model with this truncation is useful for the qualitative analysis of the most important eigenfrequencies with the largest growth rate. Since the oscillating zonal mean wind does not influence the growth rate, we set $A = 0$, and introduce the following notation for combined parameters:

$$\alpha = \gamma k^2 |B|^2, \qquad \alpha_0 = \gamma k^2 B_0^2,$$
$$\omega_G = v_G - \nu, \quad \omega_T = v_T - \nu. \tag{4.1}$$

By setting the determinant of the coefficients in (2.12) equal to zero we obtain

$$(\omega_G \omega_T - \alpha_0)\{(\omega_G + \mu)(\omega_T + \mu) - \alpha_0\} \times \{(\omega_G - \mu)(\omega_T - \mu) - \alpha_0\} = F, \tag{4.2}$$

with

$$F = 2\alpha\{2\omega_G^2 \omega_T^2 - \mu^2(\omega_G^2 + \omega_T^2)\} - 4\alpha^2 \omega_G \omega_T + 4\alpha\alpha_0\mu^2 + 4\alpha\alpha_0(\alpha - \alpha_0), \tag{4.3}$$

where all terms involving B are summarized in F. The equation is sixth order in ν and it is difficult to obtain the exact solution in analytical form, but the following successive approximation may be useful to obtain the approximate analytical result.

If $\alpha = 0$, (4.2) reduces to the classical characteristic equation. Among the six solutions we chose a pair of solutions given by

$$\omega_G \omega_T = \alpha_0. \tag{4.4}$$

Regarding this solution as the first approximation we may write the second approximation for (4.2) as

$$\omega_G \omega_T = \alpha_0 + F/[\{(\omega_G + \mu)(\omega_T + \mu) - \alpha_0\} \times \{(\omega_G - \mu)(\omega_T - \mu) - \alpha_0\}]. \tag{4.5}$$

By evaluating the right-hand side of (4.5) with the use of (4.4), we obtain

$$\omega_G \omega_T = \alpha_0 + \frac{2\alpha(v_G - v_T)^2}{\mu^2 - \mu_0^2}, \tag{4.6}$$

where we have written

$$\mu_0^2 = (v_G - v_T)^2 + 4\gamma k^2 B_0^2. \tag{4.7}$$

Although there are four more solutions for (4.2), eq. (4.6) alone is informative enough to interpret the results shown in Figs. 6–9.

The solution of (4.6) is given by

$$\nu = (v_G + v_T)/2 \pm \sqrt{S}, \tag{4.8}$$

where

$$S = \mu_0^2 + \frac{8\gamma k^2 |B|^2 (v_G - v_T)^2}{\mu^2 - \mu_0^2}. \tag{4.9}$$

The last term in (4.9) represents the effect of periodically changing zonal mean thermal wind, which enhances the instability of the basic stationary zonal mean thermal wind under the following conditions.

Suppose that the stationary zonal mean thermal wind is by itself unstable against small perturbation whose wavenumber is in the range given by (2.22). Since $\mu_0^2 < 0$ and $\gamma < 0$ the last term in (4.9) is always negative regardless of the frequency of μ, and therefore increases the growth rate of the perturbation. However, the effect of the oscillating zonal mean thermal wind becomes small when $k \to 0$, $\mu \to \infty$, or $B_0 \to \infty$, i.e., if the zonal wavelength of the perturbation is very long, the oscillation is very fast, or the basic stationary thermal wind is very strongly unstable, the effect of oscillating thermal wind is negligible.

Next, suppose that the stationary component of the thermal wind is stable against a small perturbation

$$\mu_0^2 > 0.$$

It may be proved that

$$S < 0 \tag{4.10}$$

when

$$\mu^2 < \mu_0^2, \tag{4.11}$$

$$|B|^2 > \frac{\mu_0^2(\mu_0^2 - \mu^2)}{8|\gamma|(v_G - v_T)^2}, \tag{4.12}$$

at the same time, where

$$\gamma > -\frac{(v_G - v_T)^2}{4k^2 B_0^2}. \tag{4.13}$$

Equations (4.10)–(4.12) imply that a stable stationary zonal mean thermal wind becomes unstable if an oscillating zonal mean thermal wind with a slow frequency (4.11) and with an amplitude given by (4.12) is superimposed. They imply also that with this oscillating thermal wind superimposed, the exponentially growing waves may be present in the wavenumber domain outside (2.22).

Lastly, when

$$\mu^2 = \mu_0^2 \tag{4.14}$$

(4.9) becomes very large. The divergence of the solution to infinity has apparently arisen from the undue truncation of higher harmonics which should contribute the redistribution of perturbation energy and thereby suppress the instability. We may therefore conjecture that the maximum growth rate seen in Figs. 6 and 7 is due to the matching of μ with the condition (4.14). In fact, the frequency shown by an arrow in the figure agrees with the frequency given by (4.14). For heuristic purposes, let us further put $\alpha_0 = 0$ in (4.6), giving

$$(\nu_G - \nu)(\nu_T - \nu) = \frac{2\alpha(\nu_G - \nu_T)^2}{\mu^2 - (\nu_G - \nu_T)^2}. \tag{4.15}$$

If $\alpha = 0$, (4.15) produces the independent solutions $\nu = \nu_G$ and $\nu = \nu_T$, which represent the frequency of stable neutral geopotential and temperature waves propagating in the horizontally isothermal atmosphere, respectively. Equation (4.15) indicates that with the presence of oscillating zonal mean thermal wind, these geopotential and temperature waves become interactive and the interaction is strongest when

$$\mu = \pm (\nu_G - \nu_T). \tag{4.16}$$

To interpret this simple result we return to the original governing equations (2.1) and (2.2). These are simultaneous equations for ϕ and ψ, but ϕ is involved in (2.1) only coupled to U_T, and ψ appears in (2.2) similarly only coupled to U_T. Thus we may regard $U_T \nabla^2 \phi_x$ and $U_T(\nabla^2 \psi_x + \lambda \psi_x)$ as apparent external forcing in the respective equations. Since ψ and ϕ tend to oscillate with the free frequencies ν_G and ν_T respectively, the total frequency of the forcing $U_T \nabla^2 \phi_x$ in (2.1) is $\mu + \nu_T$, and $U_T(\nabla^2 \psi_x + \lambda \psi_x)$ oscillates with frequency $\mu + \nu_G$ in (2.2). Since these source terms have the same spatial structure of the free geopotential and temperature waves, resonance is possible when

$$\nu_G = \mu + \nu_T \tag{4.17}$$

for (2.1) and

$$\nu_T = \mu + \nu_G \tag{4.18}$$

for (2.2). These resonance conditions are combined together in the single equation (4.16). In conclusion, the additional instability generated by the oscillating thermal wind is largely due to the resonance between the geopotential and temperature waves, modified by the nonlinear redistribution of energy into higher harmonics, and by the presence of a stationary thermal wind in the basic state.

5. Conclusions

In this paper we have analyzed the baroclinic instability of a zonal mean state which changes periodically with time. Due to nonlinear coupling of the frequency of the basic state and the frequency of the Rossby wave, the system generates a number of Rossby waves dispersed around the central frequency. The primary role of the changing zonal mean thermal wind is to enhance the growth rate of the unstable wave, but the phase speed of the unstable wave is also modulated considerably when the thermal wind changes with high frequency. The changing zonal mean wind does not produce any additional instability by itself but it modulates the phase velocity of unstable waves around the phase velocity predicted by the classical baroclinic instability theory. The broadening of the phase velocity is approximately proportional to the amplitude of oscillation of the zonal mean wind. The analysis suggests that when the basic state is changing with time the system may grow Rossby waves which have characteristics different from those predicted by classical baroclinic instability theory.

In the present analysis we have prescribed the zonal mean state changing with time without specifying its dynamical cause. Although a detailed discussion on the cause was not within the scope of the present study a few possibilities should be mentioned. First of all, the growing Rossby waves discussed here transport momentum and heat, which may influence the time change of the zonal mean state (Pedlosky, 1979). However, the growing baroclinic Rossby waves with wavelength comparable to the Rossby radius deformation are generally under the strong influence of nonlinear interactions with disturbances of various scales (Charney 1971). The baroclinic instability of the zonal mean thermal wind is the major energy source which maintains the geostrophic turbulence (Sasamori and Melgarejo, 1978). If the mixing of heat and momentum by the geostrophic turbulence controls the zonal mean state, the approximate time change must be governed by a diffusion equation which, however, hardly produces periodic changes in the zonal mean state with time, unless the

external source is periodically variable. The horizontal baroclinic adjustment discussed by Stone (1978) is essentially an internal and non-periodic adjustment toward an equilibrium at which the eddy heat transport by the geostrophic turbulence suppresses the baroclinicity of the zonal mean state which, at the same time, continually supplies the potential vorticity into the eddy motions. Although the baroclinic adjustment in midlatitudes is the most important process which maintains the meridional temperature gradient at the marginal instability, it seems unlikely to produce the quasi-periodic changes as shown in Fig. 1.

If the basic stationary state of the atmosphere is not horizontally homogeneous, the transient Rossby waves generate the momentum and heat fluxes through coupling with the statistically stationary waves in the atmosphere (Madden, 1975). In a separate project we have made a statistical analysis using the tropospheric data during winter, which indicates a high correlation (with a period about 20 days) between the periodical time changes of the meridional gradient of the zonal mean temperature and the heat flux generated by the coupling of the transient and quasi-stationary waves. The result of our analysis compares favorably with a theoretical model for the interaction of zonal mean flow, stationary and transient Rossby waves discussed in recent papers by Frederiksen (1978) and Sasamori and Youngblut (1981).

6. Acknowledgement

The funds for this study were provided by the National Science Foundation through grant ATM-8020738 to the University of Illinois.

REFERENCES

Charney, J. G. 1947. The dynamics of long waves in a baroclinic westerly current. *J. Meteor. 4*, 135–162.

Charney, J. G. 1971. Geostrophic turbulence. *J. Atmos. Sci. 28*, 1087–1095.

Eady, E. T. 1949. Long waves and cyclone waves. *Tellus 1*, 33–52.

Frederiksen, J. S. 1978. Instability of planetary waves and zonal flows in two-layer models on a sphere. *Quart. J. Roy. Meteorol. Soc. 104*, 374–390.

Gill, A. E. 1974. The stability of planetary waves on an infinite β-plane. *Geophys. Fluid Dyn. 6*, 26–47.

Haltiner, G. J. 1971. *Numerical weather prediction.* New York: Wiley, Inc., 317 pp.

Hirota, I. 1971a. Excitation of planetary Rossby waves in the winter stratosphere by periodic forcing. *J. Meteorol. Soc. Japan 49*, 439–449.

Hirota, I. 1971b. On the response of forced Rossby waves to the time change of zonal wind and forcing. *J. Meteorol. Soc. Japan*, Special Issue, *49*, 545–552.

Holton, J. R. 1972. *An introduction to dynamic meteorology.* New York: Academic Press, 319 pp.

Lin, C. A. 1980. Eddy heat fluxes and stability of planetary waves: Parts I and II. *J. Atmos. Sci. 37*, 2353–2380.

Lorenz, E. N. 1972. Barotropic instability of Rossby wave motion. *J. Atmos. Sci. 29*, 258–264.

Madden, R. A. 1975. Oscillation in the winter stratosphere: Part 2. The role of horizontal eddy heat transport and the interaction of transient and stationary planetary-scale waves. *Mon. Wea. Rev. 103*, 717–729.

Matsuno, T. 1971. A dynamical model for the stratospheric sudden warming. *J. Atmos. Sci. 28*, 1479–1494.

Pedlosky, J. 1979. *Geophysical fluid dynamics.* New York: Springer Verlag, 624 pp.

Phillips, N. A. 1954. Energy transformations and meridional circulations associated with simple baroclinic waves in a two-level quasi-geostrophic model. *Tellus 6*, 273–286.

Sasamori, T. and Melgarejo, J. W. 1978. A parameterization of large-scale heat transport in midlatitudes. Part I. Transient eddies, *Tellus 30*, 289–299.

Sasamori, T. and Youngblut, C. E. 1981. The nonlinear effects of transient and stationary eddies on the winter mean circulation. Part II. The stability of stationary waves. *J. Atmos. Sci. 38*, 87–96.

Stone, P. 1978. Baroclinic adjustment. *J. Atmos. Sci. 35*, 561–571.

Tung, K. K. 1976. On the convergence of spectral series—a reexamination of the theory of wave propagation in distorted background flows. *J. Atmos. Sci. 33*, 1816–1820.